

Cure Characterization of Unsaturated Polyester Resin by Near-IR and Mid-IR Spectroscopy

Bradley L. Grunden and Chong Sook Paik Sung*

Polymer Program, Department of Chemistry, Institute of Materials Science, University of Connecticut, 97 North Eagleville Road, Storrs, Connecticut 06269-3136

Received October 2, 2002; Revised Manuscript Received February 21, 2003

ABSTRACT: A near-IR spectroscopic technique for cure characterization of unsaturated polyester resin has been developed, first by using model compound mixtures to identify and quantify various reactions and then by applying these quantification techniques to the resin, with IR spectroscopy as a complementary technique. Analysis of NIR spectra of model compound mixtures (styrene/ethylbenzene, diethyl fumarate/diethyl succinate) showed that the integrated peak areas at 1629 and 2087 nm could be used to quantify the changes in the concentration of styrene and vinylenic C=C bonds in the unsaturated polyester resin, respectively. NIR-based conversions were compared with those values using mid-IR spectroscopy. Differences in NIR and mid-IR conversion values have been explained by the sample volume and heat buildup differences in the samples used to obtain the NIR and mid-IR measurements. NIR results also confirmed an optimum temperature for the highest overall conversion and vinylenic conversion, probably due to the reduced diffusion of styrene into tightly cross-linked microgels at high temperature. The complex trend of styrene conversion as a function of vinylenic conversion at 75 °C, analyzed by NIR, can be approximated by taking into account the reactivity ratios in the copolymerization reaction.

Introduction

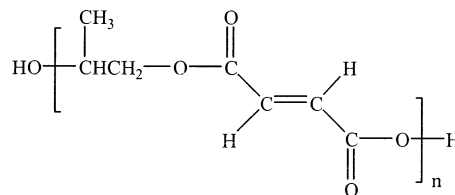
Future growth of advanced polymer applications will require development of a scientific foundation for process control. A major step in obtaining this technology will be the development of techniques capable of in-situ measurements to monitor the state of cure. Several in-situ measurement techniques have been developed to monitor the complete curing cycle of various polymers including microdielectrometry,^{1,2} ultrasonic and acoustic analysis,^{3–5} fiber optics,^{6,7} dynamic or vibration based analysis,^{8,9} fiber-optic fluorescence,^{10,11} and UV/vis¹² spectroscopy.

Our laboratory has been particularly active in the development of fluorescence, phosphorescence, and UV/vis reflection techniques based on intrinsic spectral changes for the cure monitoring in epoxy,¹³ polyimide,¹⁴ bis(maleimide),¹⁵ polyurethane and poly(urea-urethane),¹⁶ vinyl polymers,¹⁷ and polycyanurate.¹⁸

Near-infrared (NIR) spectroscopy is another analytical technique capable of monitoring the curing reaction of thermosetting polymers. Since fused silica is transparent in this region of the spectrum (780–2500 nm), this technique also readily lends itself to in-situ monitoring via fiber optics. NIR spectroscopy has previously been utilized to monitor numerous polymerization reactions including ethylene,¹⁹ styrene,^{19,20} methyl methacrylate,¹⁹ isoprene,²⁰ and epoxy resins,²¹ but not in multicomponent unsaturated polyester (UPE) resins.

The curing reaction of an unsaturated aliphatic polyester made from propylene glycol and maleic anhydride (see Scheme 1 for chemical structure) is a heterogeneous, cross-linking copolymerization via free radical chain growth between unsaturated polyester molecules and a low molecular weight monomer, typically styrene.²² Three different types of bonds can be formed during copolymerization, since reaction can occur between styrene–polyester vinylenic, polyester vinylenic–polyester vinylenic, and styrene–styrene moieties.

Scheme 1. Molecular Structure of Unsaturated Polyester Resin



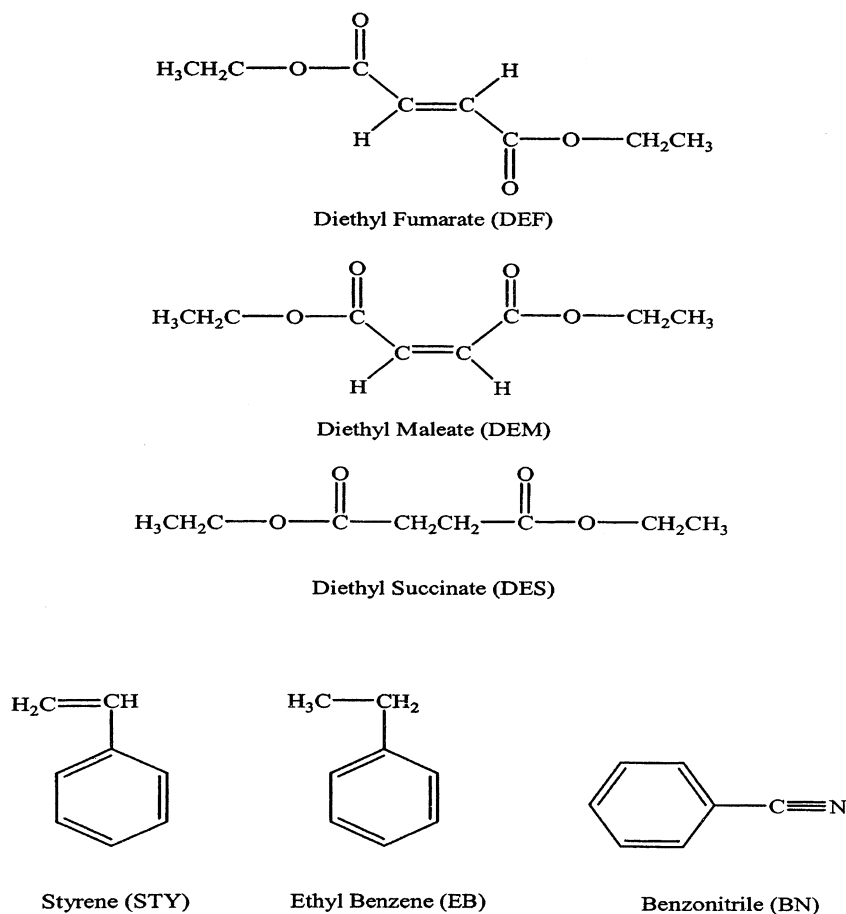
Various techniques^{22,23} such as DSC, FTIR, light scattering, rheometry, microscopy, and electron spin resonance spectroscopy have been used to characterize the cure reactions, which include induction, microgel formation, transition with or without phase separation, macrogelation, and postgelation.

The objective of this research is to develop NIR as the characterization technique for the bulk curing reaction of UPE resin with styrene, first by using model compounds to identify and quantify various reactions and to subsequently quantify the cure reaction in UPE resins. Mid-IR spectroscopy will be used to complement the NIR spectroscopic technique. The cure reactions analyzed by NIR will be explained in view of the complexities of the kinetics–gelation mechanism and by taking into account the reactivity ratios of styrene and diester in the copolymerization reaction.

Experimental Section

A. Materials. 1. Unsaturated Polyester Resin. The resin, Aropol Q6585, from Ashland Chemical Co. is a propylene glycol/maleic anhydride based unsaturated polyester cut to ~71% solids in styrene monomer. The unsaturated polyester molecules possess a number-average molecular weight (M_n) of 1580 g/mol, resulting in approximately 10 vinylenic bonds per molecule.^{22b} On the basis of these characteristics, the molar ratio of vinylenic C=C bonds/styrene C=C bonds in the resin was calculated to be 1.24. ¹H NMR spectroscopy was performed on the unsaturated polyester ground resin in CDCl₃ using a Bruker DMX-500 MHz NMR spectrometer. Quantitative analy-

Scheme 2. Chemical Structures of Model Compounds and Benzonitrile Used as an Internal Reference



sis of the integrated peak areas revealed a 1:1 molar ratio of fumarate ester:propylene glycol. This is presumably due to the fact that the *cis*-maleate ester moiety isomerizes extensively into the less strained, more planar *trans*-fumarate configuration during the synthesis of unsaturated polyester resins.^{22e} The molecular structure of the unsaturated polyester resin used in this study is shown in Scheme 1. Bulk polymerization of the unsaturated polyester was thermally induced by dissolving benzoyl peroxide (2 wt %) as the initiator in the unsaturated polyester resin by mechanical stirring for 1 h. The resin/initiator mixture was subsequently degassed under vacuum for approximately 2 min prior to curing, followed by isothermal cure in a convection oven at 60, 75, or 125 °C using a batchwise sampling technique for a predetermined time interval. The sample was allowed to cool to room temperature before recording either the NIR or mid-IR spectra.

2. Model Compounds. Diethyl fumarate (98%, ACROS Chemical Co.), diethyl maleate (98%, Aldrich Chemical Co.), diethyl succinate (99%, Aldrich Chemical Co.), styrene (99%, Aldrich Chemical Co.), ethylbenzene (99%, ACROS Chemical Co.), and benzonitrile (ACROS Chemical Co.) were used to prepare model compound reference mixtures. The chemical structures of the model compounds used in this study are shown in Scheme 2. Reference mixtures of diethyl fumarate (DEF) and diethyl succinate (DES), diethyl maleate (DEM) and diethyl succinate, and styrene (STY) and ethylbenzene (EB) were prepared in varying molar ratios for the purpose of assigning peaks in the NIR region. The molar ratios of DEF:DES, DEM:DES, and STY:EB used were 1.00:0.00, 0.80:0.20, 0.60:0.40, 0.40:0.60, 0.20:0.80, and 0.00:1.00. Benzonitrile (BN), which is a liquid, was added to liquid reference mixtures to result in miscible solution, as an internal standard to account for any thickness differences in mid-IR samples, by normalizing the peak intensities to the benzonitrile $\text{C}\equiv\text{N}$ peak at 2229 cm^{-1} . The concentration of benzonitrile in the reference mixtures was maintained at 25 mol % due to weak intensity

at 2229 cm^{-1} . However, it did not affect the absorption of other references. The same solutions containing BN were used in NIR where BN has no absorption. Model compound mixtures of DEF, DES, STY, and EB were also prepared to simulate the cure reaction of the unsaturated polyester resin. The initial ratio of DEF:STY in the reference mixtures was 1.24, the same as the vinylene/styrene double bond ratio found in the unsaturated polyester resin used in this study. A total of 36 reference mixtures were prepared by varying the degree of unsaturation in the diester component, vinyl component, or both. This was accomplished by adjusting the amount of DEF/DES:STY/EB present in the mixtures, while maintaining the initial diester:vinyl molar ratio of 1.24.

B. Instrumentation. A Perkin-Elmer UV/vis/NIR Lambda 900 spectrometer was used for all near-infrared (NIR) measurements. Sample preparation for NIR measurements consisted of placing either resin or reference mixture between two fused silica plates (1 in. diameter from Quartz Plus) with a 2.87 mm thick silicone rubber spacer.

Mid-infrared measurements were made using a Nicolet 60SX Fourier transform infrared (FTIR) spectrometer with a resolution of 4 cm^{-1} . After degassing the resin/initiator mixture, a small drop of resin was sandwiched between two NaCl crystals.

Results and Discussion

A. Assignment of NIR Absorbance Peaks. Preliminary studies during cure of unsaturated polyester with styrene revealed a decrease in peak absorbance values at 1629, 2088, 2117, and 2227 nm .²⁴ To assign these peaks to specific functional groups, model compound mixtures were analyzed.

Figure 1a shows the NIR spectra obtained for several styrene/ethylbenzene model compound mixtures. Ben-

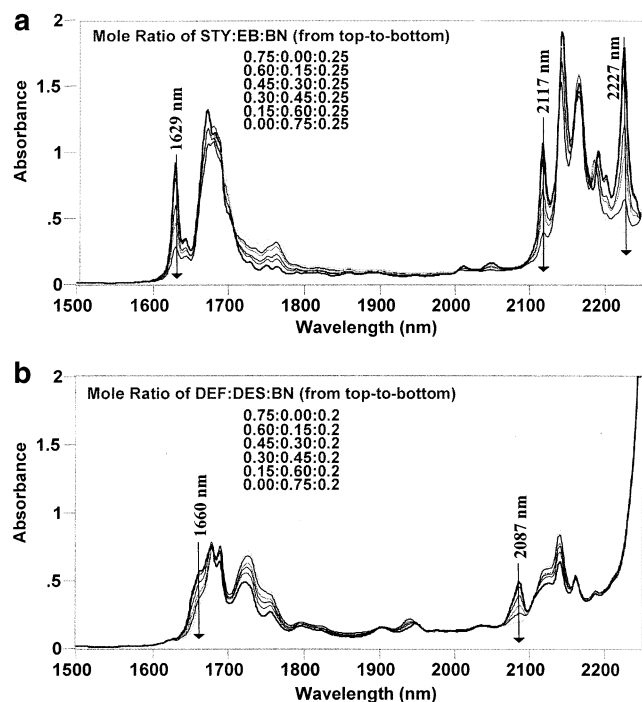


Figure 1. NIR spectra of styrene (STY)/ethylbenzene (EB) model compound mixtures (a) and diethyl fumarate (DET)/diethyl succinate (DES) mixtures (b). BN was added for mid-IR internal reference but does not have NIR absorbance in the region shown.

zonitrile in the mixture does not show significant absorbance in the NIR region of interest. A decrease in the relative molar concentration of styrene in the mixtures resulted in a decrease in the peak absorbance values at 1629, 2117, and 2227 nm. The fundamental modes of vibration responsible for these peaks were determined by analyzing the mid-IR spectra for the styrene/ethylbenzene mixtures. Absorbance peaks²⁵ at 3083 cm^{-1} (terminal methylene C–H stretching), 1630 cm^{-1} (C=C stretching), 1413 cm^{-1} (CH_2 scissoring deformation), 991 cm^{-1} (trans C–H out-of-plane bending in $\text{CH}_2=\text{CHR}$), and 908 cm^{-1} (CH_2 out-of-plane bending in $\text{CH}_2=\text{CHR}$) also decreased with decreasing styrene concentration. Considering only the frequency of the fundamental vibrations which showed a decrease in absorbance with decreasing styrene concentration, the positions of several overtone and/or combination bands were predicted. The first overtone of the terminal methylene C–H stretching vibration in styrene, ignoring the effects of anharmonicity, would be expected to occur at approximately twice the frequency of the fundamental vibration, $2 \times 3083\text{ cm}^{-1} = 6166\text{ cm}^{-1} = 1622\text{ nm}$. Since overtone bands due to fundamental transitions originating below 2000 cm^{-1} are rarely observed in the NIR due to the low probability of such transitions occurring, we would not expect any other overtone bands to be present.

However, combination bands involving the terminal methylene C–H stretching vibration were predicted at $3083 + 1630\text{ cm}^{-1} = 4713\text{ cm}^{-1} = 2122\text{ nm}$ and $3083 + 1413\text{ cm}^{-1} = 4496\text{ cm}^{-1} = 2224\text{ nm}$ derived from its combination with the C=C stretching vibration and $-\text{CH}_2$ scissoring deformation, respectively. From the mid-IR peak assignments, predicted NIR absorbance peaks, and the observed absorbance peaks in the NIR region of the spectrum, we assigned the peak at 1629 nm to the first overtone of the terminal methylene C–H

stretching vibration in styrene. The peaks observed at 2117 and 2227 nm were concluded to be the combination bands due to the combination of the terminal methylene C–H stretching with C=C stretching and $-\text{CH}_2$ scissoring deformation, respectively. Goddu²⁶ and Chang and Wang¹⁹ reported similar peak assignments for styrene in their studies. Table 1 summarizes the mid-IR and NIR peak wavelengths and assignments for styrene monomer found in this study.

NIR spectra obtained for the diethyl fumarate/diethyl succinate model compound mixtures are shown in Figure 1b. A decrease in the NIR peak at approximately 2087 nm as well as near 1660 nm was observed with decreasing diethyl fumarate concentration in the mixtures. From the mid-IR spectra for the diethyl fumarate/diethyl succinate model compound mixtures, we noted that several mid-IR peaks decreased with decreasing diethyl fumarate concentration, including peaks at 3077 cm^{-1} (C–H stretching vibration), 1646 cm^{-1} (C=C stretching vibration), 980 cm^{-1} (trans $\text{RHC}=\text{CHR}$ out-of-plane bending), and 775 cm^{-1} (trans out-of-phase wagging).²⁵ While the C–H stretching vibration at 3077 cm^{-1} is weak, analysis of the integrated peak area at this frequency was found to be linear with diethyl fumarate concentration. On the basis of the mid-IR spectra, the first overtone of the C–H stretching vibration would be predicted to occur at $2 \times 3077\text{ cm}^{-1} = 6154\text{ cm}^{-1} = 1625\text{ nm}$, while a combination of the C–H stretching with the C=C stretching vibration would be expected to appear at approximately $3077 + 1646\text{ cm}^{-1} = 4723\text{ cm}^{-1} = 2117\text{ nm}$. However, the NIR spectra of the diethyl fumarate/diethyl succinate model compound mixtures showed a shoulder at 1662 nm and a peak at 2087 nm which decreased with decreasing double bond concentration. Therefore, the assignment of these two peaks to the first overtone of the C–H stretching vibration and a combination of C–H stretching and C=C stretching would most likely be invalid. Further analysis of higher order harmonics (overtones) and combination bands involving these harmonics revealed that a combination of the second overtone of the trans $\text{RHC}=\text{CHR}$ out-of-plane bending mode at 980 cm^{-1} with the C–H stretching vibration at $3 \times 980\text{ cm}^{-1} + 3077\text{ cm}^{-1} = 6017\text{ cm}^{-1} = 1662\text{ nm}$ would be the most likely explanation for the disappearance of the shoulder at 1660 nm. Additional experimental evidence comes from the fact that the NIR spectra of the diethyl maleate/diethyl succinate model compound mixtures did not possess a shoulder which decreased with decreasing diethyl maleate concentration at 1660 nm, nor did the mid-IR spectrum possess a peak at 980 cm^{-1} associated with the trans $\text{RHC}=\text{CHR}$ out-of-plane bending vibrational mode.

The NIR spectra of both diethyl fumarate/diethyl succinate and diethyl maleate/diethyl succinate mixtures exhibited the disappearance of the peak at 2087 nm with decreasing double bond concentration in the mixtures. Since the C–H stretching vibration occurred at different frequencies, 3077 and 3060 cm^{-1} for diethyl fumarate and diethyl succinate, respectively, the combination of the C–H stretching vibration with the C=C stretching vibration would also occur at different wavelengths and thus would not explain the occurrence of the peak at 2087 nm observed in the NIR spectrum of both compounds. While diethyl fumarate and diethyl maleate are conformers of the same compound, they share only two common bands in the mid-IR region of

Table 1. Styrene NIR Peak Assignments Based on Mid-IR Spectra of Styrene/Ethylbenzene Model Compound Mixtures

wavenumber (cm ⁻¹)	fundamental vibration ²⁵	predicted NIR wavelength	observed NIR wavelength (nm)	NIR peak assignment
3083	terminal methylene C–H stretching	$2 \times 3083 = 6166 \text{ cm}^{-1} = 1622 \text{ nm}$	1629	first overtone of C–H stretching vibration
3083	terminal methylene C–H stretching	$3083 + 1630 = 4713 \text{ cm}^{-1} = 2122 \text{ nm}$	2117	combination of C–H and –C=C– stretching vibrations
1630	–C=C– stretching			
3083	terminal methylene C–H stretching	$3083 + 1413 = 4496 \text{ cm}^{-1} = 2224 \text{ nm}$	2227	combination of C–H stretching and –CH ₂ scissoring deformation
1413	–CH ₂ scissoring deformation			

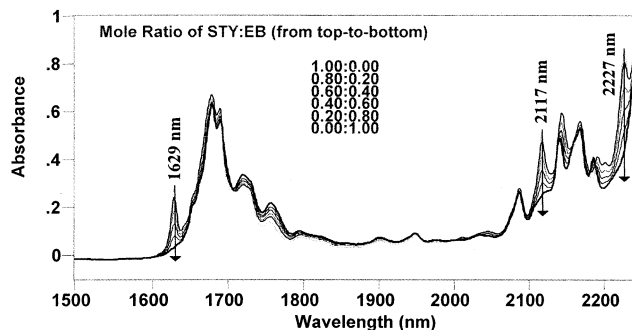
Table 2. Diethyl Fumarate NIR Peak Assignments Based on Mid-IR Spectra of Diethyl Fumarate/Diethyl Succinate Model Compound Mixtures

wavenumber (cm ⁻¹)	fundamental vibration ²⁵	predicted NIR wavelength	observed NIR wavelength (nm)	NIR peak assignment
3077	C–H stretching	$3077 + 3 \times 980 \text{ cm}^{-1} = 6017 \text{ cm}^{-1} = 1662 \text{ nm}$	1660	combination of C–H stretching and trans C–H out-of-plane bending
980	trans C–H out-of-plane bending			
1646	–C=C– stretching	$3 \times 1646 \text{ cm}^{-1} = 4938 \text{ cm}^{-1} = 2025 \text{ nm}$	2087	second overtone of –C=C– stretching vibration

the spectrum which were observed to decrease with decreasing double bond concentration. These peaks are located at 1646 cm^{-1} (–C=C– stretching) and 1300 cm^{-1} (C–H rocking).²⁵ The second overtone of the –C=C– stretching vibration, ignoring the effect of anharmonicity, would be expected to occur at approximately $3 \times 1646 \text{ cm}^{-1} = 4938 \text{ cm}^{-1} = 2025 \text{ nm}$. However, the effect of anharmonicity on the second overtone band of the –C=C– stretching vibration would cause it to appear at a frequency less than 3 times the fundamental frequency, resulting in an increase in the wavelength at which it would appear, such as at 2087 nm, a reasonable value according to the literature.²⁷ This would, therefore, explain the difference in the predicted wavelength (2025 nm) and the observed wavelength (2087 nm) for the diethyl fumarate/diethyl succinate model compounds as well as to account for the observance of the peak in the diethyl maleate/diethyl succinate model compounds. Table 2 summarizes the NIR peak assignments for diethyl fumarate.

B. Analysis of Extent of Reaction by NIR and Mid-IR. To determine the extent of styrene and vinylene reaction from the NIR spectra during cure, the spectra of model compound mixtures of known concentrations were evaluated using the initial molar ratio of diethyl fumarate: styrene monomer in the model compound mixtures of 1.24, which is the same molar ratio of vinylene to styrene double bonds in the commercial unsaturated polyester resin used in this study. The relative amounts of unsaturated diester and styrene in the mixtures were adjusted by adding appropriate amounts of diethyl succinate and ethylbenzene to simulate the disappearance of double bonds in both the unsaturated polyester and styrene components of the resin.

In Figure 2, the initial concentration of diethyl fumarate was held constant at the molar ratio of 1.24 for diester/styrene while the styrene concentration in the mixtures varied from 100 to 0 mol %. From Figure 2, it is noted that the absorbance peaks at 1629, 2117, and 2227 nm associated with styrene monomer decreased with decreasing styrene concentration. Spectral changes were quantified using the first overtone of the terminal methylene C–H stretching vibration at 1629

**Figure 2.** NIR spectra of styrene (STY)/ethylbenzene (EB) mixture with diethyl fumarate concentration constant.

nm. This peak was selected on the basis of the fact that the resolution was better than the combination peaks at 2117 and 2227 nm, thus reducing the influence of overlapping peaks on the calculated conversion. A plot of the peak absorbance or the integrated peak area at 1629 nm vs concentration was linear.

The NIR spectra were obtained for the model compound mixtures with the initial concentration of styrene held constant at the molar ratio of 1.24 for diester/styrene, and the concentration of diethyl fumarate varied from 100 to 0 mol %. The NIR absorption peak at 2087 nm attributed to the second overtone of the –C=C– stretching vibration in diethyl fumarate decreased with lowering concentration. A plot of the peak absorbance at 2087 nm or the integrated peak area at 2087 nm with concentration was also linear.

A plot of the calculated vs actual conversion of styrene and vinylene in the mixtures determined based on changes in integrated peak area is shown in parts a and b of Figure 3, respectively, exhibiting a strong linear relationship.

From the mid-IR spectra of the model compound mixtures, the conversion of styrene and vinylene C=C bonds was calculated by the method²⁸ similar to Yang and Lee²⁹ using the styrene band at 912 cm^{-1} and the polyester band at 1646 cm^{-1} . Figure 4 shows the calculated conversion of styrene and vinylene C=C bonds determined as a function of the actual conversion in the model compound mixtures. There is excellent agreement between the calculated and actual conversion

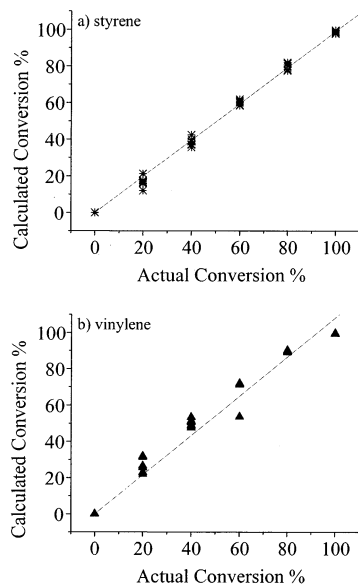


Figure 3. Plot of calculated conversion vs actual styrene conversion (a) and vinylene conversion (b) in model compound mixtures based on NIR integrated peak area.

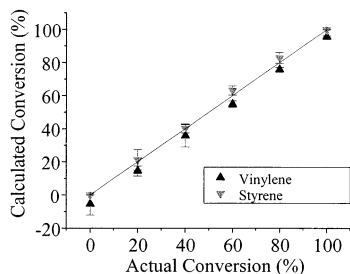


Figure 4. Plot of calculated vs actual conversion of styrene and vinylene C=C bonds in model compound mixtures determined from mid-IR measurements.

values for both styrene and vinylene components, when analyzed by mid-IR spectroscopy.

C. Isothermal Cure of Unsaturated Polyester Resin. The bulk copolymerization reaction of the Q6585 UPE resin was followed by both NIR and mid-IR spectroscopies at 60, 75, or 125 °C. Results of the NIR and mid-IR measurements at 75 °C are shown in parts a and b of Figure 5, respectively. As expected from the results of the model compounds study, the NIR spectra exhibited a decrease in absorbance at 1629, 2087, 2117, and 2227 nm with cure reaction. The changes in the NIR spectra at 1629 and 2087 nm were used to quantify the styrene and vinylene conversion and compared to conversion values calculated from the mid-IR measurements.

Figure 6a shows styrene conversion as a function of cure time determined using the two techniques for three different cure temperatures. As shown in Figure 6a, the shape of the styrene conversion profiles was found to be similar for both techniques at all three cure temperatures. However, the time for the onset of styrene reaction was earlier for the NIR samples compared to the mid-IR samples for the reactions carried out at 60 and 75 °C, which correspond to the oven temperatures, but not at 125 °C, where the increased reaction rate resulted in the cure reaction reaching about 90% within the first sampling time interval of 5 min. An explanation for this behavior may come from the differences in two samples used for each measurement. Samples used for

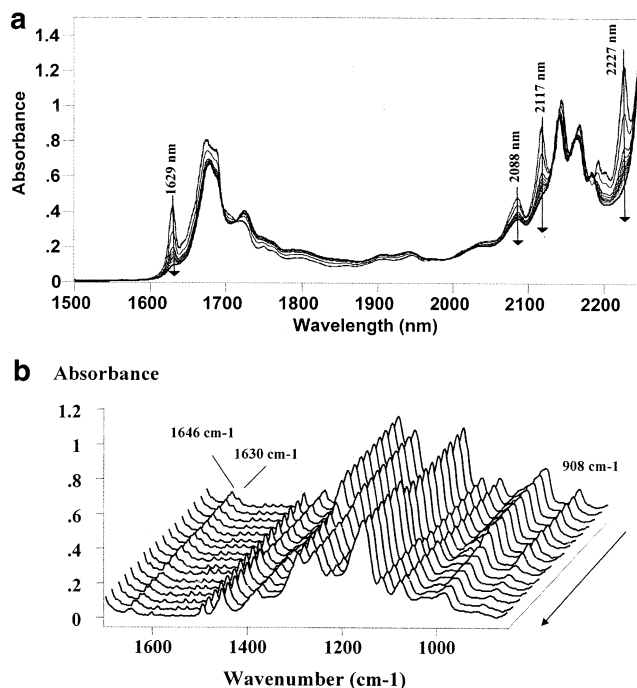


Figure 5. (a) NIR spectra and (b) mid-IR spectra of unsaturated polyester resin during cure at 75 °C (from top to bottom: $t = 0, 5, 10, 15, 20, 25, 30, 40, 50, 60, 80, 100, 120, 150, 180, 240, 480$ min).

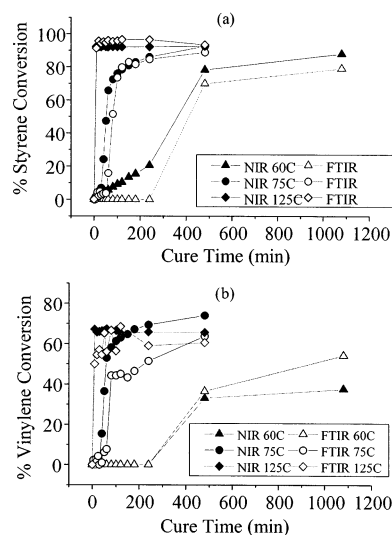


Figure 6. (a) Styrene conversion and (b) vinylene conversion as a function of cure time determined from NIR and FTIR measurements at three different cure temperatures.

NIR measurements were 2.87 mm thick with a volume of approximately 1 mL of unsaturated polyester resin, while the mid-IR samples were on the order of several microns in thickness. This would result in the NIR samples possessing approximately 400 times the volume of the mid-IR samples. Because of the exothermic nature of the free-radical copolymerization process, the increased volume in the NIR samples would allow for a greater heat buildup in the sample, thus accelerating the onset of conversion, resulting in the higher NIR styrene conversion values compared to the mid-IR styrene conversion values for the UPE resin cured at 60 and 75 °C. The measurement of the sample temperature during cure would have verified this explanation. The glass transition temperature of the similar resin

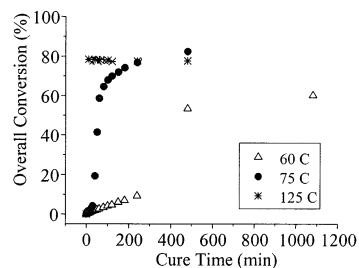


Figure 7. Overall conversion as a function of cure time for unsaturated polyester resin cured at three different temperatures from NIR data.

Table 3. Final Overall Conversion, Styrene Conversion, and Vinylene Conversion for Q6585 UPE Resin Cured at 60, 75, and 125 °C by NIR Analysis

temp (°C)	styrene conversion, α_s	vinylene conversion, α_E	overall conversion, α_T
60	88	38	60
75	93	74	82
125	93	66	78

was reported to be around 116–120 °C.²³ Therefore, at 125 °C, the styrene conversion reaches 95%, while at 75 and 60 °C, the styrene conversion values are much lower due to vitrification.

Vinylene conversion as a function of cure time for the three different cure temperatures is shown in Figure 6b. In general, the NIR vinylene conversion values were found to be higher than the mid-IR vinylene conversion values except for the resin cured at 60 °C, due to excess heat buildup in NIR samples, thus facilitating the reaction of unsaturated polyester C=C bonds.

Figure 7 shows the overall conversion, α_T , as defined by eq 1^{28,29} determined from NIR measurements as a function of cure time for the resin cured at 60, 75, and 125 °C.

$$\alpha_T = \frac{\alpha_s + 1.24\alpha_E}{2.24} \quad (1)$$

where α_s and α_E are the styrene conversion and polyester conversion, respectively. The first cure data at 125 °C corresponds to 5 min of cure in Figure 7. Table 3 displays the overall conversion, α_T , and the individual conversion of styrene and polyester vinylene groups, α_s and α_E , for the three temperatures employed. Both the overall conversion and the vinylene conversion appear to go through a maximum with an increase in temperature, since all the conversions at 75 °C are the highest, in comparison to 60 and 125 °C. Our mid-IR results showed a similar trend, which has also been reported by IR by Huang and Chen^{30a} for the resin with the molar ratio of 1.0 vinylene C=C bonds/styrene C=C bonds. They postulated that at high temperature, such as at 125 °C, enhanced microgel formation and microgel cross-linking would result in highly overlapped microgels, thus making styrene diffusion more difficult to react with polyester, lowering both overall conversion and vinylene conversion.

It is important to compare the conversion of styrene with vinylene C=C bonds in order to understand the reaction mechanism and the resulting network structure. Figure 8 reveals such a plot for the resin cured at 75 °C, where the diagonal dashed line represents the azeotropic reaction (rates of change for both styrene and vinylene C=C bonds are same). From Figure 8, styrene

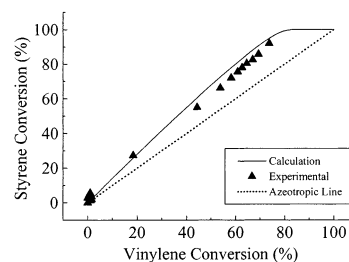


Figure 8. Comparison of experimental data and calculated data using eqs 3 and 4 for styrene conversion as a function of vinylene conversion.

conversion for the first 5% occurs early in the reaction with little or no vinylene conversion. After approximately 5% conversion, the relative rates of styrene and vinylene conversion are roughly the same up to about 50% conversion. Following 50% conversion, the conversion of styrene is slightly favored.

The relative conversion of styrene vs polyester vinylene has been reported previously for a number of different resin systems, cure temperatures, and molar ratios of styrene to polyester C=C bonds. However, there are no reports in the literature for a molar ratio (MR) of styrene to vinylene C=C bonds of 0.81, as used in this study. Huang and co-workers^{30b,c} reported that the relative conversion of styrene to polyester vinylene falls at or below the azeotropic reaction line, during the early stages of reaction for a UPE resin with MR = 1.0. The relatively faster consumption of styrene in the early stages (the first 5–7% conversion) of the reaction, as observed experimentally in Figure 8, is reasonable if one considers the monomer reactivity ratios for this system. The monomer reactivity ratio, r , is defined as the ratio of the rate constant for a propagating species adding its own type of monomer to the rate constant for its addition of the other monomer. In this system, we assumed that the monomer reactivity ratios reported for diethyl fumarate, $r_{DEF} = r_1 = 0.07$, and styrene, $r_{styrene} = r_2 = 0.30$ at 60 °C,³¹ to be applicable at 75 °C. The overall degree of conversion ($1 - M/M_0$) can be related to changes in the comonomer feed composition by eq 2.³²

$$1 - \frac{M}{M_0} = 1 - \left[\frac{f_1}{(f_1)_0} \right]^\alpha \left[\frac{f_2}{(f_2)_0} \right]^\beta \left[\frac{(f_1)_0 - \delta}{f_1 - \delta} \right]^\gamma \quad (2)$$

where the zero subscripts denote initial quantities and the other symbols are given by the following equations:

$$\alpha = \frac{r_2}{1 - r_2} \quad \beta = \frac{r_1}{1 - r_1}$$

$$\gamma = \frac{1 - r_1 r_2}{(1 - r_1)(1 - r_2)} \quad \delta = \frac{1 - r_2}{2 - r_1 - r_2}$$

M and M_0 are the combined concentrations of the two monomers at time t and the initial time, and therefore $(1 - M/M_0)$ is the overall degree of conversion. The feed composition, f_1 and f_2 , refer to that of diethyl fumarate and styrene, respectively. On the basis of the definition for conversion, we can derive separate expressions for the conversion of diethyl fumarate (DEF) and styrene as eqs 3 and 4,^{17a} respectively.

$$\text{DEF conversion} = 1 - \frac{[M_1]_t}{[M_1]_0} = \frac{(f_1)_0 - f_1 \left[1 - \left(1 - \frac{M}{M_0} \right) \right]}{(f_1)_0} \quad (3)$$

$$\text{styrene conversion} = 1 - \frac{[M_2]_t}{[M_2]_0} = \frac{(f_2)_0 - f_2 \left[1 - \left(1 - \frac{M}{M_0} \right) \right]}{(f_2)_0} \quad (4)$$

Since styrene conversion is experimentally faster than diethyl fumarate conversion, we can assume that f_1 increases with conversion, from its initial value of 0.55 to 1.00, and can calculate the overall conversion according to eq 2. Once the overall conversion is determined, we can apply eqs 3 and 4 to calculate the conversion of DEF and styrene, respectively. The solid line in Figure 8 shows the calculated styrene and diethyl fumarate conversion along with the experimental results found for the Q6585 resin cured at 75 °C. From Figure 8, one can see that the calculated and experimental conversion values agree reasonably well, suggesting that cyclization/microgelation may not occur substantially at 75 °C cure.

Summary

NIR spectra of styrene/ethylbenzene mixtures exhibited decreases in absorbance at 1629, 2117, and 2227 nm, while the NIR spectra of the diethyl fumarate (DEF) and diethyl succinate (DES) mixtures showed a decrease in an absorbance peak at 2087 nm with decreasing levels of unsaturation. On the basis of the NIR and mid-IR spectra of the styrene/ethylbenzene model compound mixtures, the NIR peaks at 1629, 2117, and 2227 nm were assigned to the first overtone of the terminal C–H stretching vibration, a combination of C–H stretching vibration and –C=C– stretching vibrations, and a combination of C–H stretching and –CH₂ scissoring deformations, respectively. From the DEF/DES model compound mixtures, the NIR peak at 2087 nm was assigned to the second overtone of the –C=C– stretching vibration.

Analysis of the NIR spectra of model compound mixtures showed that the integrated peak areas at 1629 and 2087 nm could be used to quantify changes in the concentration of styrene and diethyl fumarate, respectively. This method was applied to calculate the extent of reaction of styrene and vinylenic C=C bonds in the unsaturated polyester resin, in comparison to the extent of reaction values determined using a conventional mid-IR method. Differences in the conversion of styrene and vinylenic C=C bonds could be explained by differences in the geometry of the samples used for obtaining the NIR and mid-IR measurements.

Increasing the cure temperature resulted in an increase in the conversion of styrene, but the conversion of vinylenic C=C bonds and the overall conversion exhibited a maximum with increasing temperature, probably due to reduced diffusion of styrene into tightly cross-linked microgels. The complex trend of styrene conversion as a function of vinylenic conversion at 75 °C can be approximated by taking into account the

reactivity ratios of styrene and diethyl fumarate in the copolymerization. Since the NIR technique has the ability to measure spectra of thicker samples, which simulate the bulk state reaction of unsaturated polyester resins and composites used in the manufacturing process, it may provide an increased understanding of the curing behavior of unsaturated polyester resins, especially with the use of conventional silica grade fiber optics, which are transparent to NIR radiation.

References and Notes

- (1) Shepard, N. F.; Garverick, S. L.; Day, D. R.; Senturia, S. D. *Natl. SAMPE Symp.* **1981**, 26, 65.
- (2) Kranbuehl, D. E.; Kingsley, P. J.; Levy, D.; Williamson, A.; Hart, S. M. *SPE Antec '91 Conf. Proc.* **1991**, 941.
- (3) Gibbs, P. A. J.; Rides, M.; Williamson, P. *NPL Rep. DMM(A) (U.K., Natl. Phys. Lab., Div. Mater. Metrol.)* **1993**, DMM(A) 114, 18 pp.
- (4) White, S. R.; Mather, P. T. *Compos. Polym.* **1991**, 4, 403.
- (5) Chow, A. W.; Berlin, J. L. *Polym. Eng. Sci.* **1993**, 32, 671.
- (6) Zimmerman, B.; DeVries, M.; Claus, R. *Proceedings of Conference in Optical Fiber Sensor Based Smart Materials Structure* **1991**, 177.
- (7) Druy, M. A.; Young, P. R.; Stevenson, W. A.; Compton, D. A. *C. SAMPE J.* **1989** (May/April), 25(2).
- (8) Jang, B. Z.; Shelby, D.; Hsieh, H. B.; Lin, T. L. *Int. SAMPE Technol. Conf.* **1987**, 19, 265.
- (9) Jang, B. Z.; Shelby, D.; Hsieh, H. B. *Polym. Compos.* **1991**, 12, 66.
- (10) Sung, N. H.; Dang, W.; Paik, J. J.; Sung, C. S. P. *Int. SAMPE Symp.* **1991**, 36, 1461.
- (11) Levy, R. L.; Schwab, S. D. *Polym. Compos.* **1991**, 12, 96.
- (12) Yu, J. W.; Sung, C. S. P. *Macromolecules* **1995**, 28, 2506.
- (13) (a) Song, J. C.; Sung, C. S. P. *Macromolecules* **1993**, 26, 4818. (b) Song, J. C.; Sung, C. S. P. *Macromolecules* **1995**, 28, 5581.
- (14) (a) Pyun, E.; Mathisen, R.; Sung, C. S. P. *Macromolecules* **1989**, 22, 1174. (b) Dickinson, P.; Sung, C. S. P. *Macromolecules* **1992**, 25, 3758. (c) Kailani, M. H.; Sung, C. S. P. *Macromolecules* **1998**, 31, 5771. (d) Kailani, M. H.; Sung, C. S. P. *Macromolecules* **1998**, 31, 5779.
- (15) (a) Phelan, J. C.; Sung, C. S. P. *Macromolecules* **1997**, 30, 6837. (b) Phelan, J. C.; Sung, C. S. P. *Macromolecules* **1997**, 30, 6845.
- (16) (a) Sun, X. D.; Sung, C. S. P. *Macromolecules* **1996**, 29, 3198. (b) Wang, S. K.; Sung, C. S. P. *Macromolecules* **2002**, 35, 877. (c) Wang, S. K.; Sung, C. S. P. *Macromolecules* **2002**, 35, 883.
- (17) (a) Kim, Y. S.; Sung, C. S. P. *J. Appl. Polym. Sci.* **1995**, 57, 363. (b) Grunden, B.; Kim, Y. S.; Sung, C. S. P. *ACS Polym. Prepr.* **1996**, 37, 477.
- (18) (a) Xu, Y. E.; Sung, C. S. P. *ACS Polym. Prepr.* **1996**, 37–2, 208. (b) Xu, Y. E.; Sung, C. S. P. *ACS Polym. Prepr.* **1995**, 36–2, 356. (c) Xu, Y. E.; Sung, C. S. P. *Macromolecules* **2002**, 35, 9044. (d) Xu, Y. E.; Sung, C. S. P. *Macromolecules* **2003**, 36, 2553.
- (19) Chang, S. Y.; Wang, N. S. In *Multidimensional Spectroscopy of Polymers*; Urban, M. W., Provder, T., Eds.; American Chemical Society: Washington, DC, 1995; Chapter 9, p 147.
- (20) Long, T. E.; Liu, H. Y.; Schell, B. A.; Teegarden, D. M.; Uerz, D. S. *Macromolecules* **1993**, 26, 6237.
- (21) George, G. A.; Cole-Clarke, P.; St. John, N.; Friend, G. *J. Appl. Polym. Sci.* **1991**, 42, 643.
- (22) (a) Hsu, C. P.; Lee, L. J. *Polymer* **1993**, 34, 4516. (b) Hsu, C. P.; Lee, L. J. *Polymer* **1993**, 34, 4496. (c) Hsu, C. P.; Lee, L. J. *Polymer* **1993**, 34, 4506. (d) Tollens, F. R.; Lee, L. J. *Polymer* **1993**, 34, 29. (e) Selley, J. In *Encyclopedia of Polymer Science and Engineering*, 2nd ed.; Mark, H. F., Bikales, N. M., Overberger, C. G., Menges, G., Kroschwitz, J. I., Eds.; Wiley-Interscience: New York, 1998; Vol. 12.
- (23) Lee, D. S.; Han, C. D. *J. Appl. Polym. Sci.* **1987**, 34, 1235.
- (24) Grunden, B.; Sung, C. S. P. *ACS Polym. Prepr.* **1998**, 39–1, 248.
- (25) Lin-Vien, D.; Colthup, N. B.; Fately, W. G.; Graselli, J. G. In *Handbook of Infrared and Raman Characteristic Frequencies of Organic Molecules*; Academic Press: San Diego, CA, 1991.
- (26) Goddu, R. F. *Anal. Chem.* **1957**, 29, 1790.
- (27) Osborne, B. G.; Fearn, T.; Hindle, P. H. In *Practical NIR Spectroscopy with Application in Food and Beverage Analysis*; Wiley: New York, 1993.
- (28) Grunden, B. L. In Ph.D. Dissertation, Cure Characterization of An Unsaturated Polyester Resin Using Near-IR, Fluores-

- cence and UV/Visible Reflection Spectroscopies, University of Connecticut, 1999; pp 73–75.
- (29) Yang, Y. S.; Lee, L. J. *Macromolecules* **1987**, *20*, 1490.
- (30) (a) Huang, Y. J.; Chen, C. J. *J. Appl. Polym. Sci.* **1992**, *46*, 1573. (b) Huang, Y. J.; Chen, C. J. *J. Appl. Polym. Sci.* **1993**, *48*, 151. (c) Huang, Y. J.; Leu, J. S. *Polymer* **1993**, *34*, 295.
- (31) Grenly, R. Z. In *Polymer Handbook*, 3rd ed.; Brandrup, J., Immergut, E. H., Eds.; Wiley-Interscience: New York, 1989; Chapter II, pp 153–266.
- (32) (a) Myer, V. E.; Lowery, G. G. *J. Polym. Sci.* **1965**, *A3*, 2843. (b) Myer, V. E.; Chan, R. K. S. *J. Polym. Sci.* **1968**, *C25*, 11. (c) Dionisio, J. M.; O'Driscoll, K. F. *J. Polym. Sci., Polym. Lett. Ed.* **1979**, *17*, 701.

MA021547W